XLIII CILAMCE
21–25, November, 2022
FOZ DO IGUAÇU – PR – BRAZIL

Linear and non-linear analysis of space trusses subjected to wind actions and temperature variation

Lucas A. de Aguiar[1], Marcos B. Guimarães[1], Daniele K. Monteiro[1], Rodolfo S. da Conceição[2]

[1]*Department of Civil Engineering, Federal University of Rio Grande do Sul*
Av. Osvaldo Aranha, 99, 90035-190, Rio Grande do Sul, Brazil
lucas.a.aguiar@hotmail.com, bressan.marcos@hotmail.com, danielekauctz@hotmail.com
[2]*Department of Civil Engineering, Federal Institute of Sergipe*
Av. Eng. Gentil Tavares, 1166, 49055-260, Sergipe, Brazil
rodolfo.conceicao@ifs.edu.br

Abstract. The structural analysis seeks to determine the behavior of a structure when subjected to external actions and makes it possible to obtain its responses in terms of stresses, strains, or displacements, for example. Most engineering structures present a linear elastic behavior, however, some complex structures, such as arches and tall buildings, may present a non-linear behavior, requiring tools that allow considering such effects to obtain more realistic results. In this context, the present work proposes a comparative analysis between linear and non-linear responses in space trusses through a computer program developed in Fortran language. The structure studied is a metallic lattice dome subject to self-weight loading, wind action, and temperature variation, considering the technical specifications of the ABNT NBR 6120:2019 and ABNT NBR 6123:1988. To describe the behavior of the structure it was used the finite element formulation for bar element and the geometric nonlinearity due to normal forces. The results showed that the internal forces on the bars can vary up to 850% between the analyzed cases.

Keywords: space trusses, wind load, temperature load, nonlinear analysis, linear analysis.

1 Introduction

Space trusses are being increasingly used in the civil construction, mainly as roofing in large works. Its main advantages in relation to other structural solutions are high rigidity, low weight, the possibility of prefabrication, and ease of transport and assembly. To analyze the internal forces of this type of structure, one must seek to faithfully represent its behavior. Therefore, the lowest possible degree of simplification is sought, adopting hypotheses that focus on the characteristics of the equilibrium equation and compatibility conditions of the structure.

In most cases, these structures are calculated through linear static analysis, in which the ideal truss model is adopted, i.e., the nodes are considered as perfect hinges and ideal bars without initial imperfections and residual stresses. However, the linear analysis does not consider eccentricities, temperature variations, stresses from the assembly, section variations at the ends of the bars, and the type of node used in the structure. These factors can significantly influence the structural response of the bars, whether in the distribution of internal forces or in the calculation of displacements. Hence, the non-linear analysis reflects better the real conditions of the structure, and two types of non-linearity can be considered: the geometric one, where the calculation is performed in the displaced position of the structure; and the physical one, which considers the non-linear behavior of the material in the stress/strain ratio [1].

Therefore, this work aims to verify the behavior of a lattice dome through a linear and non-linear analysis subjected to self-weight load, temperature variation, and wind action. With the results obtained, the structural behavior is compared for each loading case.

2 Methodology

This work studied a domed roof (Fig. 1) presented by Ribas [2]. The structure has height of 9 m and radius of 15 m, all bars have Young's modulus E = 210 GPa and cross-sectional area equal to 15 cm². It was also considered that all bars have an outer diameter Φ_o = 8.0 cm and inner diameter Φ_i = 6.7 cm.

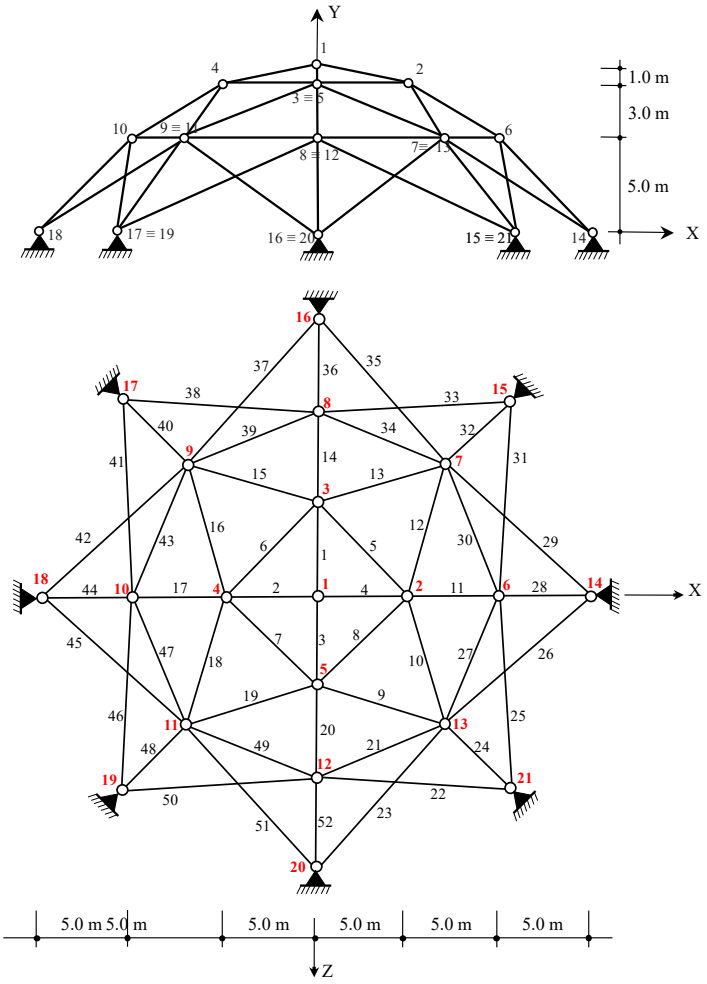

Figure 1. Lattice dome geometry

The problem analyzed was solved through a computational routine developed in FORTRAN language. The bar finite elements analysis was based on the Displacement Method for the calculation of the stiffness matrix, force vector, and displacement vector referring to the degrees of freedom of the structure. The input data has been entered in a common text file containing the coordinates of the nodes, the connectivity of the bars, the material properties, concentrated forces, and boundary conditions. Based on this information, the problem analysis process begins.

2.1 Linear analysis

The matrix calculation of the structure starts from the premise of the linear equilibrium equation (eq. (1)), where the force vector F is directly related to the stiffness matrix K and the displacement vector U.

$$F = K \cdot U \tag{1}$$

The assembly of the global stiffness matrix is performed considering the location and connectivity of each of the element nodes. For each element, the contribution to structure's global stiffness matrix (K) is computed by performing a pre and post-multiplication of the local stiffness matrix of the bars K_L by the transposed rotation matrix R^T and rotation matrix R, according to eq. (2) and eq. (3). Through the coordinates is possible calculate the length L and the directional cosines C_x, C_y and C_z, with which the rotation matrix R is assembled, as stated by Mcguire and Ziemian [3].

$$K_{BG} = R^T K_L R \quad ; \quad K_L = \frac{EA}{L} \begin{vmatrix} 1 & 0 & 0 & -1 & 0 & 0 \\ 0 & 0 & 0 & 0 & 0 & 0 \\ 0 & 0 & 0 & 0 & 0 & 0 \\ -1 & 0 & 0 & 1 & 0 & 0 \\ 0 & 0 & 0 & 0 & 0 & 0 \\ 0 & 0 & 0 & 0 & 0 & 0 \end{vmatrix} \tag{2; 3}$$

After solving the eq. (1), the displacements are found and the determination of the axial forces of the bars F_{iL} is carried out by the inverse principle of the equilibrium equation. This time, the forces found F_{iG} have the global orientation, being necessary to rotate this vector to determine the axial loads, as shown in eq. (4).

$$F_{iL} = RF_{iG} = KU \tag{4}$$

2.2 Non-linear analysis

When dealing with the nonlinear behavior of deformable bodies, the strain and displacement relationships turn out to be nonlinear. As a direct consequence, the stiffness matrix for truss elements is derived by assuming the contributions of the element linear displacements to the loading increment step [4], as demonstrated in eq. (5).

$$K_L = K_e + K_g + K_1 + K_2 + K_3 \tag{5}$$

Where K_e is the elastic stiffness matrix (eq. (6)), K_g is the geometric stiffness matrix (eq. (7)), and K_1, K_2 and K_3 (eq. (8) to (10)) are the upper matrices, able to analyze the elongation and rigid body character of the truss element [5]. Martineli [6] shows the formulation used to determine these matrices in detail.

$$K_e = \frac{EA}{L_{n-1}} \begin{vmatrix} 1 & 0 & 0 & -1 & 0 & 0 \\ 0 & 0 & 0 & 0 & 0 & 0 \\ 0 & 0 & 0 & 0 & 0 & 0 \\ -1 & 0 & 0 & 1 & 0 & 0 \\ 0 & 0 & 0 & 0 & 0 & 0 \\ 0 & 0 & 0 & 0 & 0 & 0 \end{vmatrix} \quad ; \quad K_g = \frac{F_{A_{n-1}}}{L_{n-1}} \begin{vmatrix} 1 & 0 & 0 & -1 & 0 & 0 \\ 0 & 1 & 0 & 0 & -1 & 0 \\ 0 & 0 & 0 & 0 & 0 & -1 \\ -1 & 0 & 0 & 1 & 0 & 0 \\ 0 & -1 & 0 & 0 & 1 & 0 \\ 0 & 0 & -1 & 0 & 0 & 1 \end{vmatrix} \tag{6; 7}$$

$$K_1 = \frac{EA}{2L^2_{n-1}} \begin{vmatrix} \Delta u & \Delta v & \Delta w & -\Delta u & -\Delta v & -\Delta w \\ 0 & 0 & 0 & 0 & 0 & 0 \\ 0 & 0 & 0 & 0 & 0 & 0 \\ -\Delta u & -\Delta v & -\Delta w & \Delta u & \Delta v & \Delta w \\ 0 & 0 & 0 & 0 & 0 & 0 \\ 0 & 0 & 0 & 0 & 0 & 0 \end{vmatrix} \tag{8}$$

$$K_2 = \frac{EA}{2L^2_{n-1}} \begin{vmatrix} 2\Delta u & 0 & 0 & -\Delta u & 0 & 0 \\ \Delta v & \Delta u & 0 & \Delta v & -\Delta u & 0 \\ \Delta w & 0 & \Delta u & -\Delta w & 0 & -\Delta u \\ -2\Delta u & 0 & 0 & 2\Delta u & 0 & 0 \\ -\Delta v & -\Delta u & 0 & \Delta v & \Delta u & 0 \\ -\Delta w & 0 & -\Delta u & \Delta w & 0 & \Delta u \end{vmatrix} \quad ; \quad \mathrm{K}_3 = \frac{EA}{6L^3_{n-1}} \begin{vmatrix} h & -h \\ -h & h \end{vmatrix} \tag{9; 10}$$

Where:

$F_{A_{n-1}}$ – axial force applied in the previous step;

L_{n-1} – bar length in previous step;

Δu – local variation of the force acting on the X-axis of the bar;

Δv – local variation of the force acting on the Y-axis of the bar;

Δw – local variation of the force acting on the Z-axis of the bar;

$$h = \begin{vmatrix} 3\Delta u^2 + \Delta v^2 + \Delta w^2 & 2\Delta u\Delta v & 2\Delta u\Delta w \\ 2\Delta u\Delta v & 3\Delta v^2 + \Delta u^2 + \Delta w^2 & 2\Delta v\Delta w \\ 2\Delta u\Delta w & 2\Delta v\Delta w & 3\Delta w^2 + \Delta u^2 + \Delta v^2 \end{vmatrix}.$$

As in the linear analysis, is necessary to change the orientation of the bars for the global system using the same rotation matrix *R*. In the numerical implementation of non-linear analysis, the loads are applied gradually, and the displacements and axial forces are calculated for each new incremental step, consequently changing the stiffness. With the final nodal displacements (after incrementing the step of the forces), eq. (4) is used to obtain the internal axial forces in truss bars.

2.3 Structural loads

As dead load, only the self-weight of the lattice dome was considered. The weight of each bar (W_b) was calculated by the specific mass of steel. Then, the contribution of each bar was allocated to the global force vector from the force vector of each bar (F_{Wb}), according to eq. (11) and eq. (12). Where A is the cross-sectional area, L is the length of the element, g is the acceleration of gravity, and ρ is the density of the material.

$$W_b = A \cdot L \cdot g \cdot \rho \tag{11}$$

$$F_{W_b}^T = \begin{bmatrix} 0 & -\frac{W_b}{2} & 0 & 0 & -\frac{W_b}{2} & 0 \end{bmatrix} \tag{12}$$

In addition, two live loads were considered, namely: wind action and temperature variation. The wind action was calculated using the equivalent static formulation presented by ABNT NBR 6123 [7]. For this purpose, it was arbitrated the wind acting on the Z-axis (Fig. 1), with the effective area of each bar (A_{ef}) given by the projection of the element in the XY-plane (eq. 13).

$$A_{ef} = \phi_{ef} \sqrt{L_x^2 + L_y^2} \tag{13}$$

The wind's resultant force for each bar (F_{wb}) was calculated and allocated in the global force vector according to eq. (14), adopting: basic wind speed v_0, topographic factor S_1 = 1.0, roughness factor S_2 = 1.0, probabilistic factor S_3 = 1.0, and drag coefficient C_d = 1.2.

$$F_{W_b} = \frac{1}{2} \cdot \rho_{air} \cdot \left(v_0 \cdot S_1 \cdot S_2 \cdot S_3\right)^2 \cdot A_{ef} \cdot C_d \tag{14}$$

$$F_{wind}^T = \begin{bmatrix} 0 & \frac{F_{W_b}}{2} & 0 & 0 & \frac{F_{W_b}}{2} & 0 \end{bmatrix} \tag{15}$$

The temperature variation loading was implemented by eq. (16), considering a temperature variation Δt. Thus, the internal force of each bar is calculated by the sum of the effects of self-weight, wind and/or the thermal force (F_T). Where α is the coefficient of thermal expansion, Δt is the temperature variation, E is the Young's modulus of the material and A is the cross-sectional area.

$$F_T = \alpha \cdot \Delta t \cdot E \cdot A \tag{16}$$

Six load cases were analyzed:

- Case 1: linear analysis only with self-weight load;
- Case 2: non-linear analysis only with self-weight load;
- Case 3: non-linear analysis with self-weight and thermal loads with four different temperature variations;
- Case 4: non-linear analysis with self-weight and wind loads with four different velocities;
- Case 5: linear analysis with self-weight load, wind load (v_0 = 40 m/s) and thermal load (Δt = -10 ºC);
- Case 6: non-linear analysis with self-weight load, wind load (v_0 = 40 m/s) and thermal load (Δt = -10 ºC).

3 Results and discussion

After processing the 6 cases, several analyzes were performed. Regarding Case 1, it was noted that all bars had only compressive forces, but with low values. The bars close to the supports were the ones with greater forces (see Tab. 1). The results of Case 2 were nearly to Case 1, the differences were less than 1.0%, i.e., the dome has linear behavior for self-weight dispensing the non-linear analysis.

Table 1. Axial forces for self-weight – Case 1

Bars	Axial Force (kN)
1, 2, 3, 4	– 1.50
5, 6, 7, 8	– 1.23
9, 10, 12, 13, 15, 16, 18, 19	– 1.66
11, 14, 17, 20	– 2.74
21, 27, 30, 34, 39, 43, 47, 49	– 0.92
22, 25, 31, 33, 38, 41, 46, 50	– 1.79
23, 26, 29, 35, 37, 42, 45, 51	– 1.90
24, 32, 40, 48	– 4.52
28, 36, 44, 52	– 4.05

Table 2 shows the results obtained by Case 3, where there is a combination of self-weight and thermal load. Compared to the first case, the bars in the dome can suffer an increase in the modulus of the axial force of up to six times. In addition, in the same way as in Case 2, the bar elements of the structure may undergo a change from compressive to tensile stress depending on the temperature variation adopted.

Table 2. Axial forces for self-weight and thermal load – Case 3

Bars	Axial Force (kN)				Axial Force Variation (%)			
	-10°C	-5°C	+5°C	+10°C	-10°C	-5°C	+5°C	+10°C
1, 2, 3, 4	-1.51	-1.50	-1.50	-1.50	0.33	0.10	0.04	0.21
5, 6, 7, 8	-1.15	-1.19	-1.27	-1.31	-6.22	-3.14	3.20	6.45
9, 10, 12, 13, 15, 16, 18, 19	-1.81	-1.73	-1.58	-1.51	9.22	4.59	-4.54	-9.04
11, 14, 17, 20	-2.52	-2.63	-2.85	-2.96	-7.98	-4.00	4.03	8.08
21, 27, 30, 34, 39, 43, 47, 49	-6.55	-3.72	1.87	4.63	615.22	306.35	-303.78	-605.05
22, 25, 31, 33, 38, 41, 46, 50	3.79	1.00	-4.60	-7.43	-310.92	-155.82	156.55	313.80
23, 26, 29, 35, 37, 42, 45, 51	3.96	1.04	-4.85	-7.80	-308.51	-154.54	155.13	310.84
24, 32, 40, 48	-11.81	-8.16	-0.90	2.70	160.98	80.34	-80.02	-159.74
28, 36, 44, 52	-10.68	-7.36	-0.76	2.52	163.42	81.56	-81.26	-162.22

For Case 4, the results show that the axial forces can be four times greater than in Case 1. In addition, the wind load can change the type of stress in the bars, i.e., going from compression to tension, as shown in Fig. 2.

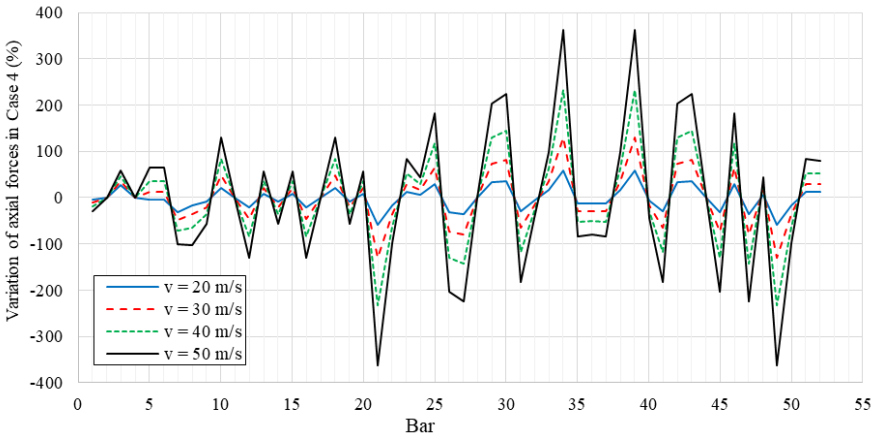

Figure 2. Axial forces for self-weight + wind load – Case 4

Figure 3 presents the results of Cases 1, 2, 5 and 6. Even with greater variation in the results of Cases 5 and 6, where a combination of self-weight load, wind load, and temperature load variation is applied, the effects of geometric nonlinearity increase the axial forces insignificantly, to a maximum of 2.0%. It is worth noting that when the structure is subjected to wind load combined with temperature variation, the internal axial forces on the truss bars increase by up to 850%. This must be observed for the correct design of the lattice dome.

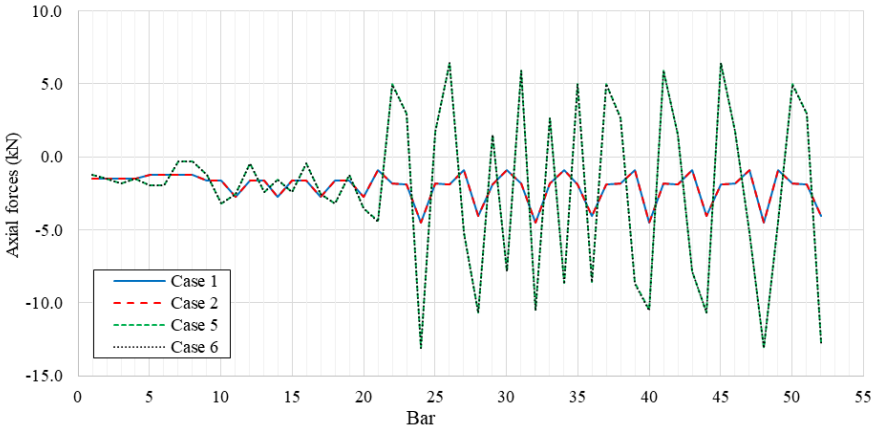

Figure 3. Axial forces for Cases 1, 2, 5 and 6

Considering a real project situation in which the actions of wind and temperature would be increased by safety factors, the structure would be considered unsafe. For example, considering the indications of ABNT NBR 8186:2003 [8] that provides values for safety factors γ to be used in the verification of structural failure, the values of 1.25, 1.20, and 1.40 are indicated for self-weight, temperature, and wind actions, respectively. It also indicated the eq. 17 to analyze the various loading conditions for n dead loads and m live loads. In this equation, one of the variable loads is considered as main (Q_1) and the other ones are considered as secondary ($Q_{2,\ 3\ \ldots\ m}$), being multiplied by a reducing factor Ψ_0 (both temperature and wind have a coefficient equal to 0.6 when secondary). Figure 4 shows the variation of axial forces in bars 3, 9, 24, and 36 obtained through eq. 17.

$$N_d = \sum_{i=1}^{n} N_{G_i} \cdot \gamma_{G_i} + N_{Q_1} \cdot \gamma_{Q_1} + \sum_{j=2}^{m} N_{Q_j} \cdot \gamma_{Q_j} \cdot \psi_{Q_j} \tag{17}$$

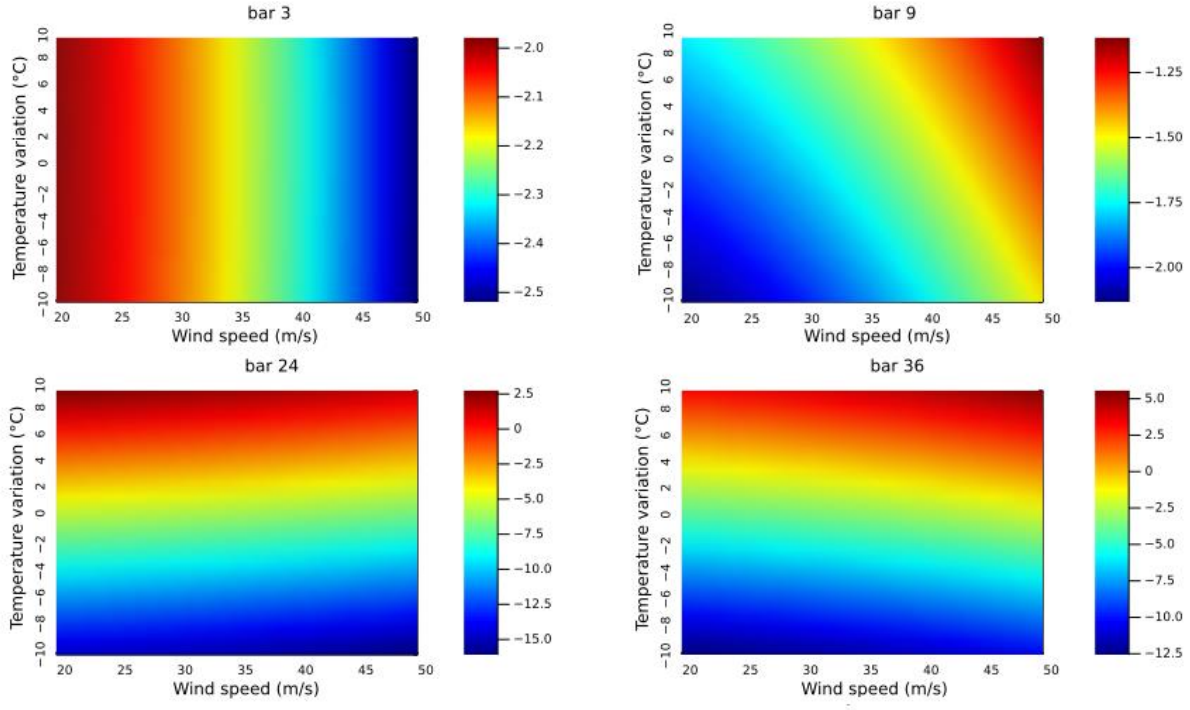

Figure 4. Design axial forces N_d (kN) for bars 3, 9, 24 and 36

As seen in Fig. 4, the consideration of variable loads must be carried out bar by bar, since for some elements the influence of temperature is more significant (e.g. bars 24 and 36), in others the action of the wind is more important (e.g. bar 3), while others both are important (e.g. bar 9). Finally, it should be noted that some bars (e.g. bars 24 and 36) should be designed for both traction and compression. And it is important to emphasize that although the internal forces (and stresses) are still relatively small considering the physical and geometric properties adopted, the base elements are at the limit for buckling since they are very slender, for bar 24, for example, the critical buckling load is equal to 13.48 kN.

4 Conclusions

Trusses are structures widely used in civil construction and are a viable solution for large spans. This is due to the fact they obtain high rigidity with reduced weight and excellent redistribution of forces. The domes, in turn, increase the load redistribution characteristics by having an arc shape.

Thus, with the results obtained in all load cases for the lattice dome, it is concluded that the variation of the axial forces in the tubular steel bars increases significantly when the structure is requested by live loads. For example, this increase can reach a variation of 850% when comparing Case 1 with Case 5. This shows the need for structural analysis in the design of trussed domes, considering all possible types of loads that a structure is subject to.

Furthermore, due to the symmetry of spherical domes, the greatest axial forces were in the bars positioned close to the support. The maximum force was 13.75 kN (compression), in the case with a combination of self-weight load, wind load, and thermal load.

Regarding the comparison between the linear and non-linear analysis solution, the results obtained were not significant enough. There was only a maximum increase of 2.0% in the axial forces when comparing Case 5 with Case 6.

Acknowledgements. The authors are grateful for the financial support provided by CAPES and the Federal Institute of Sergipe.

Authorship statement. The authors hereby confirm that they are the sole liable persons responsible for the authorship of this work, and that all material that has been herein included as part of the present paper is either the property (and authorship) of the authors or has the permission of the owners to be included here.

References

[1] A. S. C. de Souza and R. M. Gonçalvez, "Treliças Espaciais – Aspectos Gerais, Comportamento Estrutural e Informações para Projetos". Technical paper, Federal University of São Carlos and São Carlos School of Engineering, 2007.
[2] H. S. Ribas, "Projeto Ótimo da Geometria de Treliças Espaciais". Master's thesis, Federal University of Rio Grande do Sul, 1980.
[3] W. Mcguire, R. H. Gallagher and R. D. Ziemian, "Matrix Structural Analysis". New York, 2nd ed.2014.
[4] M. Sathyamoorthy, "Nonlinear analysis of structures". CRC, 2017.
[5] Y. B. Yang, S. R. Kuo, "Theory and analysis of nonlinear framed structures". New York : Prentice Hall, 1994.
[6] L. B. Martinelli, "Otimização de esruturas treliçadas geometricamente não lineares, submetidas a carregamento dinâmico". Master's thesis, Federal University of Espirito Santos, 2019.
[7] ABNT, "NBR 6123 – Forças devidas ao vento em edificações". Rio de Janeiro, 1988.
[8] ABNT, "NBR 6123 – Ações e Segurança nas Estruturas". Rio de Janeiro, 2003.